Urban Climate Changes Due to Extreme Modification of Human Behaviour During the COVID-19 Pandemic: Integration of Urban Physics with Social Big Data

Yuya Takane (takane.yuya@aist.go.jp)
National Institute of Advanced Industrial Science and Technology https://orcid.org/0000-0002-6259-2748
Ko Nakajima
National Institute of Advanced Industrial Science and Technology (AIST)
Yukihiro Kikegawa
Meisei University https://orcid.org/0000-0002-5225-653X

Article

Keywords:

Posted Date: April 1st, 2022

DOI: https://doi.org/10.21203/rs.3.rs-1341525/v1

Version of Record: A version of this preprint was published at npj Climate and Atmospheric Science on June 2nd, 2022. See the published version at https://doi.org/10.1038/s41612-022-00268-0.

Abstract

The changes in human behaviour associated with the spread of COVID-19 infections have changed the urban environment. However, little is known about the extent to which they have changed the urban climate. We quantitatively evaluated these effects using a unique method that integrates real-time human population data (social big data) with an urban climate model. The results showed that in an office district in the city centre of Tokyo, the biggest metropolis in the world, under a significantly reduced population, electricity consumption (CO_2 emissions) would be 30% and anthropogenic heat emission would be 33% of pre-COVID levels (without the stay-at-home advisories). This resulted in a temperature decrease of about 0.2°C, representing about 10% of the past greenhouse gas-induced warming in Tokyo. This method can be benchmarked and then applied to worldwide. The results suggest that changes in human behaviour can represent an adaptation strategy to climate change in cities.

Introduction

The coronavirus SARS-CoV-2 (COVID-19) pandemic significantly changed human behaviour worldwide. In many major cities globally, the ensuing lockdowns greatly restricted human activity. In Japan, a state of emergency was declared in April 2020, which reduced the daytime population in city office districts by more than 50% due to the promotion of teleworking at home (Figure S1). This change in human behaviour may continue to some extent after COVID-19, with the development of a “new-normal” situation.

Previous studies have reported how the lockdown and stay-at-home advisories have changed environments worldwide. For example, air quality has improved [1] [2] [3] [4] [5] and greenhouse gas (GHG) emissions have been reduced [6] [7] [8] [9] [10] due to lockdowns and stay-at-home advisories. Changes in the land-surface temperature due to lockdowns have also been reported [11]. In addition, the lockdown and stay-at-home advisories could have changed the urban climate in terms of urban near-surface air temperature (T), anthropogenic heat emissions (Q_F) and electricity consumption (EC) because the urban climate is strongly affected by human behaviour [12]. However, only a few studies have attempted to estimate this effect based on the local climate (e.g., [13] [14] [15]). The technical difficulty of detecting changes in urban T due to the pandemic is a limitation in such studies. From an observational perspective, it is not easy to clarify a pandemic signal (temperature change due to the stay-at-home advisories) in observed temperatures because the weather changes constantly due to natural variability. It is not possible to conclude that an urban temperature decrease/increase during lockdown was not just due to the natural variation in urban temperature.

Under such a limitation, a numerical simulation using urban parameterisations is a powerful tool, which could extract the pandemic signal. For example, urban parameterisation could estimate the impact of Q_F on urban T [16] [17] [18] [19] [20] [21] [22] [23] [24]. There is robust evidence and high agreement that urban parameterisations can be used to generally simulate radiation exchanges in a realistic way [25]. However, there is another limitation in the use of a numerical model in that due to its incomplete modelling of the relationship between urban climate and human behaviour. For example, a single-layer urban canopy model (UCM) [26] can handle the input of Q_F, which relates to human behaviour but does not directly express human behaviour (the diurnal change in Q_F is input into the model). In this study, a coupled model, UCM with the building energy model (BEM) (hereafter, UCM-BEM) [27] [14] [28] [29] was used to express human behaviour and simulate its effects on the urban climate (see the Methods section for details of how human behaviours were input into the model).

Using the UCM-BEM, a previous study attempted to estimate the impact of stay-at-home advisories due to COVID-19 on the urban climate [14]. The authors developed a simulation system that used real-time population and traffic data. More specifically, they estimated population and traffic changes due to COVID-19 and input these changes as the UCM-BEM parameters related to human behaviour. This new modelling system showed that the COVID-19 stay-at-home advisories resulted in a Q_F of 76.3 W m^{-2} and a 0.13°C air temperature reduction in urban areas in Osaka, the second-largest city in Japan. Although this work indicated the impact of COVID-19 on urban climate based on numerical simulations, there were some limitations. They did not consider the actual stay-at-home advisories period of COVID-19, and they used population change data on only one ideal office grid point in Osaka. To estimate the impact of COVID-19 on urban climate with more accuracy, it is necessary to conduct a simulation during the actual stay-at-home advisories period based on population change data for all of the grid points in a target area.

Estimations made using a numerical model are essential in areas related to global climate change, urban climate, sustainability, environment, human behaviour and urban planning. With cities predicted to be home to more than 66% of the global population by 2050 [30], urban warming due to global warming and the urban heat island effect are critical issues [31] [32] [33] [34] [35] [24] [36]. Changes in human behaviour due to lockdowns and stay-at-home advisories could be an adaptation strategy to climate change in urban areas, but it remains unclear how effective those would be. In urban areas significantly affected by climate change [25], many “hard-type” climate change adaptation strategies (traditional urban heat island mitigation techniques such as greening and cool roofs) have been proposed and evaluated [37] [35] [38]. A “soft-type” strategy, such as a change in human behaviour, has yet to be assessed sufficiently, although some studies have already estimated weekday–weekend temperature differences [39] [40] [41] [42]. The impact of changes in human behaviour on urban climate remains unknown. The COVID-19 pandemic could provide an opportunity to understand how human behaviour affects the urban climate based on scientific principles.

We estimated the impact of changes in human behaviour related to the COVID-19 pandemic on the urban climate in the world’s biggest metropolitan area of Tokyo, which has a hot and humid climate during summer, using the UCM-BEM and real-time population and traffic data (social big data). Through this sophisticated estimation, we developed simple equations to estimate the impact for the whole of Japan and other countries with similar climates, building materials and human behaviour. The aim was to understand whether changes in human behaviour could be an adaptation strategy to climate change.

Results

2.1 Changes in human behaviour due to the COVID-19 pandemic

The population densities of the Tokyo Metropolitan Area (TMA) on 18 April–14 May 2019 and 2020 (Fig. 1a and b) and its change ratio (2020/2019) (Fig. 1c) were plotted. Human activity was significantly changed by the pandemic. The population in the centre of Tokyo and its surrounding area decreased and increased, respectively (Fig. 1c). The traffic count differed from the population data. The traffic counts decreased in almost all areas of the TMA due to the stay-at-home advisories (Fig. 1f). These changes in population and traffic counts were used as human behavioural change parameters in the numerical model (see details in the Methods section).

2.2 Urban climate change in the TMA

After verification of the numerical model (see Supplementary information and Nakajima *et al.* [43]), we estimated the impact of COVID-19 induced human behavioural changes on the urban climate (Fig. 3).

We calculated the changes in EC (COVID minus No-COVID: ΔEC). The daytime (9–17 Japan Standard Time [JST]) EC in the centre of Tokyo (office area) decreased (Fig. 2a, b) due to the reduced population (Fig. 1c). For example, the number of people using the Tokyo railway station during the pandemic was only 39.4% of the pre-COVID level, and the EC during the pandemic was estimated to be 30.2% of the pre-COVID level (Table 1a). By contrast, the EC increased in residential areas (Fig. 2a, b) due to the increase in the daytime population (Fig. 1c). These ΔEC values were mainly due to changes in the baseload (EC for appliances that is not affected by changes in T) during the stay-at-home advisories period (April–May). This period was not the season when urban residents typically use space heating or cooling (Figure S1b). The EC was directly correlated with population change in terms of building use in commercial and business grids (office: hereafter, C), residential grids that predominantly consisted of fireproof apartments (Rm) and residential grids that were chiefly covered by wooden detached dwellings (Rd) (Fig. 2c). Based on the ΔEC, the changes in CO_2 emissions were estimated using the CO_2 emissions coefficient of 0.000445 (t- CO_2 kWh-1) (https://www.env.go.jp/press/files/jp/115373.pdf). The estimation showed that daily total CO_2 emissions in the 23 wards of Tokyo decreased by 8.2% (8.06 t- CO_2/km^2/day) due to the COVID-19 pandemic.

The ΔEC affected the daytime changes in Q_F (ΔQ_F). As with the ΔEC, the Q_F decreased due to the pandemic in the centre of Tokyo (Fig. 2d), with a reduction of about − 1.3 GW in the total office grids (Fig. 2e). The Q_F in the areas surrounding Rm was also reduced by a decrease in traffic (Fig. 1f). Figure 2f shows the relationship between the population change ratio and Q_F, and indicates that, as with the ΔEC, the ΔQ_F was also correlated with population change.

The ΔQ_F causes changes in the urban T (ΔT). Figure 2g shows the impact of the pandemic-induced human behavioural changes on daytime urban T and indicates that the temperature in the centre of Tokyo (C areas) decreased due to the pandemic. The temperature decrease reached − 0.21°C (Fig. 2h, Table 1a, Tokyo railway station). By contrast, there were no temperature changes in the surrounding areas (residential areas) (Fig. 2g, h). The relationship between the population change ratio and temperature change is shown in Fig. 2i, which indicates that temperature tended to decrease with population reduction in the office area (C). There was no clear relationship in the residential areas (Rd and Rm).

As in the daytime, the EC, Q_F and T were also impacted by the changes in human behaviour in the nighttime, but the impact was lower because nocturnal human behaviour during that time did not change significantly.

Table 1 Summary of the relationships between the changes in population and urban climate at seven railway stations on the Kanto Plain, including the Tokyo Metropolitan Area (TMA) (see **Figure 1f**)(**a**) and for nine major cities in Japan (see **Figure 3**)(**b**)

a

	Tokyo Sta (To)	Yokohama Sta (Yo)	Chiba Sta (Ch)	Omiya Sta (Om)	Mito Sta (Mi)	Takasaki Sta (Ta)	Utsunomiya Sta (Us)
Population (2020/2019×100, %)	39.4	50.0	66.8	79.3	86.7	80.6	83.6
EC& CO_2 (COVID/no-COVID×100, %)	30.2	37.8	56.0	73.1	72.0	67.7	75.0
Q_F(COVID/no-COVID×100, %)	32.8	62.4	65.1	82.1	79.8	77.1	83.6
ΔT (COVID – no-COVID, ºC)	−0.21	−0.08	−0.08	−0.02	0.03	−0.02	−0.01

b

	Sapporo (Hokkaido)	Sendai (Miyagi)	Tokyo (Tokyo)	Nagoya (Aichi)	Kyoto (Kyoto)	Osaka (Osaka)	Kobe (Hyogo)	Fukuoka (Fukuoka)
Population (2020/2019×100, %)	56.6	59.1	39.4	40.1	45.4	38.4	55.3	49.7
ΔEC (W floor m^{-2})	−6.7	−6.3	−12.3	−9.3	−4.2	−9.6	−6.9	−7.8
ΔQ_F (W m^{-2})	−22.5	−21.2	−75.6	−30.8	−2.7	−31.6	−23.2	−25.9
ΔT (ºC)	−0.07	−0.07	−0.21	−0.10	−0.01	−0.10	−0.07	−0.08

2.3 Application to the urban climate of all Japanese cities

Based on the detailed estimation using the model and the mobile spatial statistics (MSS) population data shown in Section 2.2, we estimated the impact of the pandemic on the urban climate for all Japanese cities. There was a clear relationship between the population change ratio (ΔP) and, ΔEC, ΔQ_F, and ΔT (Fig. 2c, f, i), which could be used to estimate the impact of COVID-19 on the urban climate of other cities. We proposed the following equations:

$$\Delta EC_{i,j,t} = a\Delta P_{i,j,t} + b \quad (1)$$

$$\Delta Q_{Fi,j,t} = c\Delta P_{i,j,t} + d \quad (2)$$

$$\Delta T_{i,j,t} = e\Delta P_{i,j,t} + f \quad (3)$$

where i and j are the grid numbers in the zonal and meridional direction, t is hours, and a (c, e) and b (d, f) are the slope and intercept, respectively (Table S2). These relationships were used for the simple estimation of the impact of COVID-19 on the urban climate of all Japanese cities. For example, it was possible to estimate the impact of changes in human behaviour on the EC of all Japanese cities using just a linear Eq. (1), actual population change

data and land-use data (urban categories: C, Rd, and Rm)(Fig. 3b) for all Japan cities. Similarly, the impact on Q_F and T could also be estimated.

Figure 3c shows the estimated ΔEC using Eq. (1) for TMA. The horizontal distribution of ΔEC (Fig. 2a) simulated by the sophisticated model was reproduced using equation (a). Based on the above, Fig. 3 and Table 1b indicate that EC decreased due to the pandemic at all major city centres in Japan. Similarly, it was possible to estimate the impact on CO_2 emissions and Q_F, with similar results to those obtained for EC (Table 1b). We developed simple equations based on the detailed simulation results, which were used to estimate the impact on cities in Japan and other countries with similar climates, building materials, lifestyles and air conditioning (AC) usage.

Discussion

3.1 Comparison with observations and previous estimations

The results of this study and previous studies are summarised in Table 2. A maximum temperature decrease of about − 0.2°C was estimated for Tokyo's office district due to the pandemic. This temperature decrease was consistent with the reported temperature decrease of about − 0.1°C in central Osaka, which was previously estimated using the same method [14]. More importantly, the calculated results were consistent with the temperature decrease in central Tokyo and cities in China previously estimated from observations and a statistical analysis (-0.40 ± 0.21°C [13] and − 0.42 ± 0.26°C [15])), which was an entirely different approach from the present study. The consistency between results suggest that ΔT could be estimated realistically.

As described in the introduction, only a few studies have evaluated ΔT induced by the COVID-19 pandemic, and comparisons with the results of previous studies are therefore limited. Instead, our results are compared to those of studies that have assessed the effects of introducing urban planning scenarios on T. Specifically, Adachi *et al.* [44] and Kusaka *et al.* [45] estimated the impact of a dispersed city, i.e., an urban planning scenario in which offices and other functions are distributed around the city centre, rather than being concentrated in the city centre. Because commuting to the city centre was significantly reduced during the state of emergency period (Fig. 1), the voluntary restraint on going out due to the pandemic could cause a similar situation in terms of commuter behaviour compared with that in a dispersed city. Therefore, we compared our results of a temperature decrease of about − 0.2°C, with those of Adachi *et al.* [44] and Kusaka *et al.* [45]. The dispersed city scenario was estimated to induce negative ΔT reaching − 0.2–0.3°C in the city centre (Table 2). Our estimate is almost the same. Thus, the stay-at-home advisories can be viewed as a kind of social experiment similar to the introduction of dispersed cities. To create a dispersed city, offices need to be moved from the city centre to the suburbs, which costs money. Promoting telework would therefore be more cost-effective than developing a dispersed city.

Furthermore, the temperature difference between weekdays and holidays was compared to the T drop of -0.2°C recorded in this study. Temperatures are lower in office areas in central Tokyo on weekends than on weekdays because fewer working people on weekend there [39] [40] [41] [46] [47]. The stay-at-home advisories could induce a situation resembling a holiday almost every day. Therefore, comparing the temperature difference between weekdays and holidays is essential. In estimates made in previous studies, the temperature on holidays was − 0.1–0.6°C lower than on weekdays (Table 2). Our values are consistent, which implies that the estimated impacts of this study are reasonable. The numerical model used in this study reproduced the difference between observed weekday and holiday temperatures well and was used for calculations in cities [48], and it was therefore reasonable to make the above comparison. Finally, Chinese New Year (CNY) influenced the impact of changes in human behaviour on T. The

impact was about − 0.6°C [49] [50] [51] [42], and therefore the impact of the stay-at-home advisories tended to be smaller than that of CNY, although the order of magnitude was comparable.

In terms of CO_2 emissions, we estimated that emissions during COVID were about 7% smaller than during the No-COVID period in the residential area of Tokyo, which qualitatively agrees with the changes in the observed CO_2 flux in the same area reported by Sugawara et al. [9].

Table 2
Summary of the results of previous studies and this study.

Target	Signal	City	Method	Ref.
Stay-at-home/lockdown	−0.2 ºC (daytime)	Tokyo, Japan	Numerical experiments	This study
	About − 0.1 ºC (daytime)	Osaka, Japan	Numerical experiments	Nakajima *et al.* [14]
	−0.40 ± 0.21 ºC (daytime) No signal	Tokyo, Japan Osaka, Japan	Observation and statistical analysis	Fujibe [13]
	−0.42 ± 0.26 ºC (daytime)	Cities in China	Observation and statistical analysis	Liu *et al.* [15]
Dispersed city scenario	About − 0.3 ºC (night-time)	Tokyo, Japan	Numerical experiments	Adachi *et al.* [44]
	−0.2 ~ 0.25 ºC (daytime)	Tokyo, Japan	Numerical experiments	Kusaka *et al.* [45]
Weekday-weekend differences	−0.2 ~ 0.25 ºC (daytime) −0.10 ~ 0.20 ºC (daytime) (weekends < weekdays)	Tokyo, Japan Osaka, Japan	Observation and statistical analysis	Fujibe [39] [40]
	−0.13 ~ 0.37 ºC (mean)	12 cities in Germany	Observation and statistical analysis	Bäumer and Vogel [46]
	−0.2 ~ 0.6 ºC (daytime) (weekends < weekdays)	Osaka, Japan	Observation and statistical analysis	Ohashi *et al.* [41]
	−0.1 ~ 0.2 ºC (09 LT) −0.1 ~ 0.4 ºC (09 LT)	Melbourne, AU Sydney, AU	Observation and statistical analysis	Earl *et al.* [47]
Mass human movements (Chinese New Year holiday)	−0.65 ºC (daily mean)	Harbin, China	Observation and statistical analysis	Wu *et al.* [49]
	−0.64 ºC (daily mean)	Beijing, China	Observation and statistical analysis	Zhang *et al.* [50]
	About − 0.6 ºC (daily mean)	Beijing, China	Observation and statistical analysis	Zhang and Wu [51]
	−0.3 ~ 0.6 ºC	Beijing, China	Observation and statistical analysis	Dou and Miao [42]

3.2 Could changes in human behaviour be a climate change adaption in urban areas?

Section 2.2 shows the urban climate change due to the pandemic in the spring season when AC is rarely used. In the future, it is likely that AC usage will increase as urban temperatures increase leading to high levels of heat stress [24] [36]. To assess the potential for climate change adaptation in cities, it was necessary to estimate how the urban climate changed due to the pandemic during summer when AC is often used. The state of emergency continued until the summer of 2020 in Japan. Therefore, we estimated the impact of COVID-19 stay-at-home advisories on the summer urban climate and compared the effect with widely adopted climate change adaptation strategies (e.g., greening and cool roofs).

Figure S2 shows the impact of the pandemic on urban climate in terms of EC (ΔEC), Q_F (ΔQ_F) and T (ΔT) during the summer period. The daytime EC in the centre of Tokyo decreased (Figure S2a) due to the population reduction (Fig. 1c) and limited AC use. By contrast, there was a large EC increase in the residential areas (Figure S2a, b) due to the daytime population increase (Fig. 1c) and high levels of AC use. This trend was supported by observations using a smart meter in residential houses in Japan (not shown). These ΔEC values were caused by changes in the baseload and AC use (Figure S2b). The EC was directly correlated with the changes in the occupancy of buildings (Figure S2c). The estimation showed that the daily total CO_2 emissions in the 23 wards of Tokyo decreased by 7.9% (11.07 t-CO_2/km^2/day) due to the COVID-19 pandemic.

The Q_F in summer decreased much more than in spring due to the pandemic in the centre of Tokyo (Figure S2d versus Fig. 2d), with the amount being about − 3.1 GW in the office grids (Figure S5e). By contrast, the Q_F in the Rm areas increased due to AC use, although the traffic count decreased (Figure S2e and Fig. 1f). Figure S2f shows the relationship between the population change ratio and ΔQ_F, which indicated that the ΔQ_F was much more strongly correlated with population change than temperature in spring (Figure S2f versus Fig. 2f).

The ΔT in the centre of Tokyo (office area) was − 0.30°C, which was a more significant impact than in spring (Figure S2h versus 2h) and was equivalent to 20% of the past greenhouse gas induced warming in Tokyo. In contrast to office areas, the temperature increased in the surrounding areas (residential areas) (Figure S2g, h). This increase was also much more significant than in spring (Figure S2h versus 2h). The relationship between the population change ratio and temperature change is shown in Figure S2i, which suggests that temperature tended to decrease/increase with population changes in the office area C and residential areas (Rd and Rm). respectively.

The magnitude of the temperature change (ΔT) may increase under future climate change because many urban residents will begin to use AC, and the thermal heat load will be increased by the increase in outdoor temperature [52] [24] [36]. The summertime ΔT presented above is comparable/similar to that attained by adopting the well-known urban heat island countermeasure techniques [37] [35] (e.g., cool roofs and greening [53]). An advantage of change in human behaviour induced by the pandemic as an adaptation strategy is that there are no/small introduction and running costs. In addition, such changes in human behaviour could reduce exposure to high-heat stress in the outdoor environment. Future studies should estimate the combined effects of this change in human behaviour (a “soft-type” strategy) and other well-known adaptation strategies, such as greening and cool roofs (a “hard-type” strategy) [37] [35].

Methods

Human behaviour and traffic data (social big data)

We used MSS data regarding the stay-at-home advisories (18 April–14 May 2020) and the same dates in 2019 (18 April–14 May 2019) provided by NTT Docomo, Inc. The MSS data provided population statistics based on the location of 78 million users of NTT Docomo's mobile terminals on whole Japan. The MSS data are created from this information [14]. First, the number of mobile terminals in each base station area was aggregated. Second, the total number of mobile terminals was extrapolated based on the adoption rates of NTT Docomo mobile terminals. Finally, the estimated population was re-aggregated into each grid section. More details of the MSS estimation method are provided by Terada *et al*. [54]. The temporal and spatial resolutions of MSS data were 1 h and 500 m, respectively. Previously, MSS data have been used to estimate human activity in urban climates [14] and human health [55]. Other population data such as location trends were provided by KDDI, Inc. and the Japan Travel Guide of NTT Advertising, Inc.; however, their sample numbers were relatively small [56]. Thus, MSS provides data that can be used to examine real-time changes in specific populations.

The level of traffic congestion is related to the Q_F derived from automobiles ($Q_{F,\,tra}$). To estimate the changes in traffic volumes during the stay-at-home advisories, we used traffic counts for public roads at 5 min intervals for 8,060 sites in TMA in April–May 2019 and 2020. These data were provided by the Japan Road Traffic Information Center and was distributed by the Japan Traffic Management Technology Association.

Model

The study used the Advanced Research WRF (ARW) ver. 3.7.1 [57] and the online coupling of WRF and CM-BEM [27] (hereafter, WRF-CM-BEM [58] [14]). Figure 6 shows the model domain that covered the area of Japan, including TMA, which was the focus of our study. The d01, d02 and d03 domains consisted of 89, 110 and 250 grid points, respectively, in the x and y directions. We set the horizontal grid spacing to 25, 5 and 1 km in the domains d01, d02 and d03, respectively. The model top was 50 hPa, with 34 vertical sigma levels. In this simulation, the initial and boundary conditions were derived from the National Centers for Environmental Prediction-National Center for Atmospheric Research (NCEP-NCAR) reanalysis data [59].

The following schemes were used in the simulation: the updated Rapid Radiation Transfer Model longwave scheme [60], the Goddard shortwave scheme [61] [62], the Thompson microphysics scheme [63], the Mellor–Yamada–Janjic (MYJ) atmospheric boundary-layer scheme [64] [65] [66], the Noah land surface model [67], and the CM-BEM [27] [58] for the TMA and for a single-layer urban canopy [26] [68] [69] in some urban grids around the city centre.

As in Takane *et al.* [21] and Nakajima *et al.* [14], building footprint (polygon) data from a geographical information system (GIS) in the TMA were used to identify if buildings were being used. The building use and total floor area for each building in the TMA was recorded. Land use and land cover (LULC) data and topographic datasets of the Geospatial Information Authority of Japan (GIAJ) were used in this study. In addition to the GIAJ LULC data, the ArcGIS Geo Suite provided by ESRI-Japan Co., Ltd. (esrij.com/products/data-content-geosuite-shosai/) and a land use survey performed in the 2016 fiscal year by the Bureau of Urban Development of the Tokyo Metropolitan Government were used for classification. The urban grids were classified into three categories (C, Rm and Rd) based on the dominant building type, as shown in Fig. 7b. In the study, when we analysed each category, we only used the grids for that category within the TMA.

The model used in this study required the identification of parameters for the detailed building energy calculations. For the geometric parameters of urban canopies, the mean building width, mean distance between buildings, and distribution of building height had to be set in every urban grid. These settings were derived from the same building

footprint data and were summarised in Table S2. For the building energy simulation, the diurnal variation in the number of occupants, and AC systems were based on the values in the literature for the three-urban categories (Figure S3). More details of the parameters are provided in previous studies [70] [58] [71] [72] [21] [24] [36]. Note that we set the EC for appliances (baseload EC) in every urban grid based on actual EC data presented by Nakajima *et al.* [14] [73].

As with Kikegawa *et al.* [58] and Nakajima *et al.* [14] [73], the hourly total consumption of motor fuels in each grid, with a temporal resolution of 1 h, was estimated using traffic census data [74] and fuel economy data [75]. The combustion heat was obtained as the $Q_{F,\,tra}$.

We also used the Automated Meteorological Data Acquisition System (AMeDAS) data for TMA (Fig. 1b) provided by the Japan Meteorological Agency (JMA) as meteorological data.

The simulation was carried out from 0900 JST (Japan Standard Time; 0000 UTC = 0900 JST) on 12 April to 0900 JST 17 May 2020 (Figure S1b). The first 5 days were discarded and considered the model spin-up. In this study, we referred to this simulation as the No-COVID case. For comparison with the April–May simulation, we conducted a summertime simulation, which ran from 0900 JST on 27 July to 0900 JST 1 September 2020 (see Section 3.2, Figure S1c). COVID-19 simulation

In addition to the No-COVID case, another case (COVID) was also conducted to estimate the impact of COVID-19 stay-at-home advisories in the city. Because the population and traffic count during the COVID case differed from those of usual days (Fig. 1), we modified the human behaviour parameters (the number of occupants, EC for appliances and AC operation schedule) and $Q_{F,tra}$ using the population change ratio of the stay-at-home advisories period to the usual days (ΔP^{COVID}) and the traffic count ratio of the stay-at-home advisories period to the usual days (Δtra). The ΔP^{COVID} and Δtra values are plotted in Fig. 1c and f, respectively. The modified human behavioural parameters (X^{COVID}) of each grid were calculated for the working hours (08.00–22.00 JST) on the stay-at-home advisories period as follows (Fig. 4):

$$X_{i,j,t}^{COVID} = X_{i,j,t}^{No-COVID} \times \Delta P_{i,j,t}^{COVID} for t = 8, 9, \ldots, 21, 22 JST$$

4

where i and j are the grid numbers in the zonal and meridional directions, respectively, t is hours and $X^{No\text{-}COVID}$ is the human behaviour parameter in the No-COVID case (see Fig. 4).

Similarly to the aforementioned parameters, the diurnal variation in $Q_{F,tra}$ in the stay-at-home advisories period ($Q_{F,\,tra}{}^{COVID}$) was calculated as follows:

$$Q_{F,\,trai,j,t}^{COVID} = Q_{F,\,trai,j,t}^{No-COVID} \times \Delta t_{trai,j,t} \quad for t = 0, 1, \ldots, 22, 23 JST$$

5

where $Q_{F,\,tra}{}^{No\text{-}COVID}$ is $Q_{F,\,tra}$ in No-COVID.

Declarations

Data availability

The downscaling data produced by the WRF were deposited in local storage at AIST. This is available from the corresponding author upon reasonable request. The source code of the WRF and forcing data that support the findings of this study are available from http://www2.mmm.ucar.edu/wrf/users/and https://rda.ucar.edu/, respectively. The observational data used in this study are available from the JMA website: https://www.jma.go.jp/jma/index.html. The population and traffic counts data are available from: https://mobaku.jp/and https://www.jartic.or.jp/service/opendata/, respectively.

Code availability

The source code of the WRF that support the findings of this study are available from http://www2.mmm.ucar.edu/wrf/users/.

Acknowledgments

This study was supported by Steel Foundation for Environmental Protection Technology Fund. We also thank the Environmental Research and Technology Development Fund (grant no. JPMEERF20191009) of the Environmental Restoration and Conservation Agency of Japan.The simulations were performed by using the supercomputer system (HPE Apollo 2000) of the National Institute for Environmental Studies (NIES).

Contributions

YT conceived the study and designed the analyses. YT and KN prepared the data for regional climate simulations, and KN conducted the simulations and analysis using the data. YT wrote the original manuscript and KN and YK provided comments, feedback, and revisions to the manuscript.

Competing interests

The authors declare no competing financial interests

References

[1] Y. Zhu, J. Xie, F. Huang and L. Cao, “Association between short-term exposure to air pollution and COVID-19 infection: Evidence from China,” Science of The Total Environment, 727, 2020.

[2] M. Bauwens, S. Compernolle, T. Stavrakou, J.-F. Müller, J. Van Gent, H. Eskes, P. F. Levelt, R. Van Der A, J. P. Veefkind, J. Vlietinck and C. Zehner, “Impact of Coronavirus outbreak on NO2 pollution assessed using TROPOMI and OMI observations,” Geophysical Research Letters, 47, 2020.

[3] P. M. Forster, H. I. Forster, M. J. Evans, M. J. Gidden, C. D. Jones, C. A. Keller, R. D. Lamboll, C. Le Quéré, J. Rogelj, D. Rosen, C.-F. Schleussner, T. B. Richardson and C. Smith, “Current and future global climate impacts resulting from COVID-19,” Nature Climate Change, 10, 2020.

[4] P. Samani, C. García-Velásquez, P. Fleury and Y. v. der Meer, "The Impact of the COVID-19 outbreak on climate change and air quality: four country case studies," Global Sustainability, 4, 2021.

[5] N. Evangeliou, S. M. Platt, S. Eckhardt, C. L. Myhre, P. Laj, L. Alados-Arboledas, J. Backman, B. T. Brem, M. Fiebig, H. Flentje, A. Marinoni, M. Pandolfi, J. Yus-Dìez, N. Prats and P, “Changes in black carbon emissions over Europe due to COVID-19 lockdowns,” Atmospheric Chemistry and Physics, 21, 2021.

[6] C. Le Quéré, R. B. Jackson, M. W. Jones, A. J. P. Smith , S. Abernethy, R. M. Andrew, A. J. De-Gol , D. R. Willis, Y. Shan, J. G. Canadell, P. Friedlingstein, F. Creutzig and G. P. Peters, “Temporary reduction in daily global CO2 emissions during the COVID-19 forced confinement,” Nature Climate Change, 10, 2020.

[7] A. J. Turner, J. Kim, H. Fitzmaurice, C. Newman, K. Worthington, K. Chan, P. J. Wooldridge, P. Köehler, C. Frankenberg and R. C. Cohen, “Observed impacts of COVID-19 on urban CO2 emissions,” Geophysical Research Letters, 47, 2020.

[8] C. D. Jones, J. E. Hickman, S. T. Rumbold, J. Walton, R. D. Lamboll, R. B. Skeie, S. Fiedler, P. M. Forster, J. Rogelj, M. Abe, M. Botzet, K. Calvin, C. Cassou and J. N. Cole, “The Climate Response to Emissions Reductions Due to COVID-19: Initial Results From CovidMIP,” Geophysical Research Letters, 48, 2021.

[9] H. Sugawara, S. Ishidoya, Y. Terao, Y. Takane, Y. Kikegawa and K. Nakajima, "Anthropogenic CO2 Emissions Changes in an Urban Area of Tokyo, Japan, Due to the COVID-19 Pandemic: A Case Study During the State of Emergency in April–May 2020," Geophysical Research Letters, 48, 2021.

[10] C. Bertram, G. Luderer, F. Creutzig, N. Bauer, F. Ueckerdt, A. Malik and O. Edenhofer, “COVID-19-induced low power demand and market forces starkly reduce CO2 emissions,” Nature Climate Change, 11, 2021.

[11] B. R. Parida, S. Bar, D. Kaskaoutis, A. C. Pandey, S. D. Polade and S. Goswami, “Impact of COVID-19 induced lockdown on land surface temperature, aerosol, and urban heat in Europe and North America,” Sustainable Cities and Society, 75, 2021.

[12] T. R. Oke, G. Mills, A. Christen and J. A. Voogt, Urban Climates, Cambridge University Press, 2017.

[13] F. Fujibe, “Temperature anomaly in the Tokyo Metropolitan Area during the COVID-19 (coronavirus) self-restraint period,” Scientific Online Letters on the Atmosphere, 16, 2020.

[14] K. Nakajima, Y. Takane, Y. Kikegawa, Y. Furuta and H. Takamatsu, "Human behaviour change and its impact on urban climate: Restrictions with the G20 Osaka Summit and COVID-19 outbreak," Urban Climate, 35, 2021.

[15] Z. Liu, J. Lai, W. Zhan, B. Bechtel, J. Voogt, J. Quan, L. Hu, P. Fu, F. Huang, L. Li, Z. Guo and J. Li, “Urban heat islands significantly reduced by COVID-19 lockdown,” Geophysical Research Letters, 49, 2022.

[16] F. Kimura and S. Takahashi, “The effects of land-use and anthropogenic heating on the surface temperature in the Tokyo Metropolitan area: A numerical experiment,” Atmospheric Environment, 25, 1991.

[17] T. Ichinose, K. Shimodozono and K. Hanaki, “Impact of anthropogenic heat on urban climate in Tokyo,” Atmospheric Environment, 33, 1999.

[18] Y. Ohashi, Y. Genchi, H. Kondo, Y. Kikegawa, H. Yoshikado and Y. Hirano, “Influence of air-conditioning waaste heat on air temperature in Tokyo during summer: numerical experiments using an urban canopy model coupled with a building energy model,” Journal of Applied Meteorology and Climatology, 46, 2007.

[19] C. De Munck, G. Pigeon, V. Masson, F. Meunier, P. Bousquet, B. Tréméac, M. Merchat, P. Poeuf and C. Marchadier, “How much can air conditioning increase air temperatures for a city like Paris, France?,”

International Journal of Climatology, 33, 2013.

[20] F. Salamanca, M. Georgescu, A. Mahalov, M. Moustaoui and M. Wang, “Anthropogenic heating of the urban environment due to air conditioning,” Journal of Geophysical Research Atmosphere, 119, 2014.

[21] Y. Takane, Y. Kikegawa, M. Hara, T. Ihara, Y. Ohashi, S. A. Adachi, H. Kondo, K. Yamaguchi and N. Kaneyasu, “A climatological validation of urban air temperature and electricity demand simulated by a regional climate model coupled with an urban canopy model and a building energy model in an Asian megacity,” International Journal of Climatology, 37, 2017.

[22] Y. Wang, Y. Li, S. D. Sabatino, A. Martilli and P. W. Chan, “Effects of anthropogenic heat due to air-conditioning systems on an extreme high temperature event in Hong Kong,” Environmental Research Letters, 13, 2018.

[23] X. Xu, F. Chen, S. Shen, S. Miao, M. Barlage, W. Guo and A. Mahalov, “Using WRF-Urban to assess summertime air conditioning electric loads and their impacts on urban weather in Beijing,” Journal of Geophysical Research Atmosphere, 123, 2018.

[24] Y. Takane, Y. Kikegawa, M. Hara and C. S. B. Grimmond, “Urban warming and future air-conditioning use in an Asian megacity: importance of positive feedback,” npj Climate and Atmospheric Science, 2, 2019.

[25] IPCC, “AR6 Climate Change 2021: The Physical Science Basis,” 2021.

[26] H. Kusaka, H. Kondo, Y. Kikegawa and F. Kimura, "A simple single-layer urban canopy model for atmospheric models: Comparison with multi-layer and slab models," Boundary-Layer Meteorology, 101, 2001.

[27] Y. Kikegawa, Y. Genchi, H. Yoshikado and H. Kondo, "Development of a numerical simulation system toward comprehensive assessments of urban warming countermeasures including their impacts upon the urban buildings' energy-demands," Applied Energy, 76, 2003.

[28] F. Salamanca, A. Krpo, A. Martilli and A. Clappier, “A new building energy model coupled with an urban canopy parameterization for urban climate simulations—part I. formulation, verification, and sensitivity analysis of the model,” Theoretical and Applied Climatology, 99, 2010.

[29] F. Salamanca and A. Martilli , “A new Building Energy Model coupled with an Urban Canopy Parameterization for urban climate simulations—part II. Validation with one dimension off-line simulations,” Theoretical and Applied Climatology, 99, 2010.

[30] D. o. E. a. S. A. United Nations, “World Urbanization Prospects: The 2014 Revision,” (ST/ESA/SER.A/366), 2015.

[31] K. Oleson, “Contrasts between Urban and Rural Climate in CCSM4 CMIP5 Climate Change Scenarios,” Journal of Climate, 25, 2012.

[32] H. Kusaka, M. Hara and Y. Takane, “Urban climate projection by the WRF model at 3–km grid increment: dynamical downscaling and predicting heat stress in the 2070’s August for Tokyo, Osaka, and Nagoya,” Journal of Meteorological Society of Japan, 90B, 2012.

[33] M. Georgescu, M. Moustaoui , A. Mahalov and J. Dudhia , “Summer-time climate impacts of projected megapolitan expansion in Arizona,” Nature Climate Change, 3, 2013.

[34] A. C. G. Varquez and M. Kanda, “Global urban climatology: a meta-analysis of air temperature trends (1960-2009),” NPJ Climate and Atmospheric Science, 1, 2018.

[35] E. S. Krayenhoff, M. Moustaoui, A. M. Broadbent , V. Gupta and M. Georgescu, “Diurnal interaction between urban expansion, climate change and adaptation in US cities,” Nature Climate Change, 8, 2018.

[36] Y. Takane, Y. Ohashi, C. S. B. Grimmond, M. Hara and Y. Kikegawa, “Asian megacity heat stress under future climate scenarios: Impact of air-conditioning feedback,” Environmental Research Communications, 2, 2021.

[37] M. Georgescu, P. E. Morefield, B. G. Bierwagen and C. P. Weaver, “Urban adaptation can roll back warming of emerging megapolitan regions,” Proceedings of the National Academy of Sciences of the United States of America, 111, 2014.

[38] N. H. Wong, C. L. Tan, D. D. Kolokotsa and H. Takebayashi , “Greenery as a mitigation and adaptation strategy to urban heat,” Nature Reviews Earth & Environment, 2, 2021.

[39] F. Fujibe, “Weekday-weekend differences of urban climates Part 1: temporal variation of air temperature,” Journal of the Meteorological Society of Japan. Ser. II, 65, 1987.

[40] F. Fujibe, “Day-of-the-week variations of urban temperature and their long-term trends in Japan,” Theoretical and Applied Climatology, 104, 2010.

[41] Y. Ohashi, M. Suido, Y. Kikegawa, T. Ihara, Y. Shigeta and M. Nabeshima, “Impact of seasonal variations in weekday electricity use on urban air temperature observed in Osaka, Japan,” Quarterly Journal of the Royal Meteorological Society, 142, 2016.

[42] J. Dou and S. Miao, “Impact of mass human migration during Chinese New Year on Beijing urban heat island,” International Journal of Climatology, 37, 2017.

[43] K. Nakajima, Y. Takane, K. Yukihiro and Y. Kazuki, “Development of a building energy model to improve the reproducibility of electricity consumption in an urban area,” Journal of advances in Modeling Earth Systems, In preparation, 2022.

[44] S. A. Adachi, F. Kimura, H. Kusaka, M. G. Duda, Y. Yamagata, H. Seya, K. Nakamichi and T. Aoyagi, “Moderation of summertime heat island phenomena via modification of the urban form in the Tokyo Metropolitan Area,” Journal of Applied Meteorology and Climatology, 53, 2014.

[45] H. Kusaka, A. Suzuki-Parker, T. Aoyagi, S. A. Adachi and Y. Yamagata, “Assessment of RCM and urban scenarios uncertainties in the climate projections for August in the 2050s in Tokyo,” Climatic Change, 137, 2016.

[46] D. Bäumer and B. Vogel, “An unexpected pattern of distinct weekly periodicities in climatological variables in Germany,” Geophysical Research Letters, 34, 2007.

[47] N. Earl, I. Simmonds and N. Tappe, “Weekly cycles in peak time temperatures and urban heat island intensity,” Environmental Research Letters, 11, 2016.

[48] Y. Kikegawa, K. Nakajima, Y. Takane, Y. Ohashi and T. Ihara, “A quantification of classic but unquantified positive feedback effects in the urban-building-energy-climate system,” Applied Energy, 307, 2022.

[49] L.-Y. Wu, J.-Y. Zhang and C.-X. Shi, “Mass human migration and the urban heat iisland during the Chinese new year holiday: A case study in Harbin city, Northeast China,” Atmospheric and Oceanic Science Letters, 8, 2015.

[50] J. Zhang, L. Wu, F. Yuan, J. Dou and S. Miao, “Mass human migration and Beijing’s urban heat island during the Chinese New Year holiday,” Science Bulletin, 60, 2015.

[51] J. Zhang and L. Wu, “Influence of human population movements on urban climate of Beijing during the Chinese New Year holiday,” Scientific Reports, 7, 2017.

[52] M. Tewari, F. Salamanca, A. Martilli, L. Treinish and A. Mahalov, “Impacts of projected urban expansion and global warming on cooling energy demand over a semiarid region,” Atmospheric Science Letters, 18, 2017.

[53] D. E. Bowler, L. Buyung-Ali , T. M. Knight and A. S. Pullin , “Urban greening to cool towns and cities: A systematic review of the empirical evidence,” Landscape and Urban Planning, 97, 2010.

[54] M. Terada, T. Nagata and M. Kobayashi, ““Mobile spatial statistics” supporting development of society and industry — population estimation technology using Mobile network statistical data and applications,” NTT Docomo Technical Journal, 14, 2013.

[55] Y. Ohashi, Y. Takane and K. Nakajima, “Impact of COVID-19 pandemic on changes in temperature-sensitive cardiovascular and respiratory disease mortality in Japan,” Nature Human Behaviour, Submitted, 2022.

[56] N. Matsubara, “Grasping dynamic population by “Mobile Spatial Statistics”: From the viewpoint of tourism disaster and stranded persons,” Journal of Information Processing and Management, 60, 2017.

[57] W. C. Skamarock, J. B. Klemp, J. Dudhia, D. O. Gill, D. M. Barker, W. Wang and J. G. Powers, “A description

of the advanced research WRF version 3," NCAR TECHNICAL NOTE, NCAR/TN–468+STR, 2008.

[58] Y. Kikegawa, A. Tanaka, Y. Ohashi, T. Ihara and Y. Shigeta, "Observed and simulated sensitivities of summertime urban surface air temperatures to anthropogenic heat in downtown areas of two Japanese Major Cities, Tokyo and Osaka," Theoretical and Applied Climatology, 117, 2014.

[59] E. Kalnay, M. Kanamitsu, R. Kistler, W. Collins, D. Deaven, L. Gandin, M. Iredell, S. Saha, G. White, J. Woollen, Y. Zhu, A. Leetmaa, R. Reynolds, M. Chelliah, W. Ebisuzaki, W. Higgins, J. Janowiak, K. C. Mo, C. Ropelewski, J. Wang and J, "The NCEP/NCAR 40-year reanalysis project," Bulletin of the American Meteorological Society, 77, 1996.

[60] E. J. Mlawer, S. J. Taubman, P. D. Brown, M. J. Iacono and S. A. Clough, "Radiative transfer for inhomogeneous atmospheres: RRTM, a validated correlated-k model for the longwave," Journal of Geophysical Research Atmosphere, 102, 1997.

[61] M.-D. Chou and M. J. Suarez, "An efficient thermal infrared radiation parameterization for use in general circulation models," NASA Technical Memorandum, 104606, 1994.

[62] T. Matsui, S. Q. Zhang , S. E. Lang, W.-K. Tao, C. Ichoku and C. D. Peters-Lidard , "Impact of radiation frequency, precipitation radiative forcing, and radiation column aggregation on convection-permitting West African monsoon simulations," Climate Dynamics, 55, 2020.

[63] G. Thompson, P. R. Field, R. M. Rasmussen and W. D. Hall, "Explicit forecasts of winter precipitation using an improved bulk microphysics scheme. Part II: Implementation of a new snow parameterization," Monthly Weather Review, 136, 2008.

[64] G. L. Mellor and T. Yamada, "Development of a turbulence closure model for geophysical fluid problems," Reviews of Geophysics, 20, 1982.

[65] Z. I. Janjić, "The step-mountain eta coordinate model: further developments of the convection, viscous sublayer, and turbulence closure schemes," Monthly Weather Review, 122, 1994.

[66] Z. I. Janjić, "Nonsingular implementation of the Mellor-Yamada level 2.5 scheme in the NCEP Meso model," NCEP Office Note, 437, 2002.

[67] F. Chen and J. Dudhia, "Coupling an advanced land surface–hydrology model with the Penn State–NCAR MM5 modeling system. Part I: model implementation and sensitivity," Monthly Weather Review, 129, 2001.

[68] H. Kusaka and F. Kimura, "Thermal effects of urban canyon structure on the nocturnal heat island: Numerical experiment using a mesoscale model coupled with an urban canopy model," Journal of Applied Meteorology and Climatology, 43, 2004.

[69] F. Chen, H. Kusaka, R. Bornstein, J. Ching, C. S. B. Grimmond, S. Grossman-Clarke, T. Loridan, K. W. Manning, A. Martilli, S. Miao, D. Sailor, F. P. Salamanca, H. Taha, M. Tewari and Wang, "The integrated WRF/urban modelling system: development, evaluation, and applications to urban environmental problems," International Journal of Climatology, 31, 2011.

[70] T. Ihara, Y. Kikegawa, K. Asahi, Y. Genchi and H. Kondo, "Changes in year-round air temperature and annual energy consumption in office building areas by urban heat-island countermeasures and energy-saving measures," Applied Energy, 85, 2008.

[71] Y. Kikegawa, Y. Yamakawa, E. Tokutake, Y. Ohashi, Y. Takane, T. Ihara and M. Nabeshima, "Validation of a numerical urban weather forecasting model coupled with a building energy model in terms of the reproducibility of solar irradiance and electricity demand," Journal of Japan Society of Civil Engineers Ser. G Environmental Research, 73, 2017.

[72] Y. Takane, S. Aoki, Y. Kikegawa, Y. Yamakawa, M. Hara, H. Kondo and S. Iizuka, "Future projection of electricity demand and thermal comfort for August in Nagoya city by WRF-CM-BEM," Journal of Environmental Engineering, AIJ, 80, 2015.

[73] K. Nakajima, Y. Takane, S. Fukuba, K. Yamaguchi and Y. Kikegawa, "Urban electricity–temperature relationships in the Tokyo Metropolitan Area," Energy and Buildings, 256, 2022.

[74] T. a. T. Japanese Ministry of Land, Infrastructure, , "Nation-wide road traffic condition study (road traffic census), Fiscal 1999," 2001.

[75] Environment Agency of Japan, “The survey result on automobile exhaust unit rate and total amounts,” 1998.

[76] W. Gemmill, B. Katz and X. Li, “Daily real-time, global sea surface temperature - high-resolution analysis at NOAA/NCEP,” NOAA/NWS/NCEP/MMAB Office Note, 260, 2007.

Figures

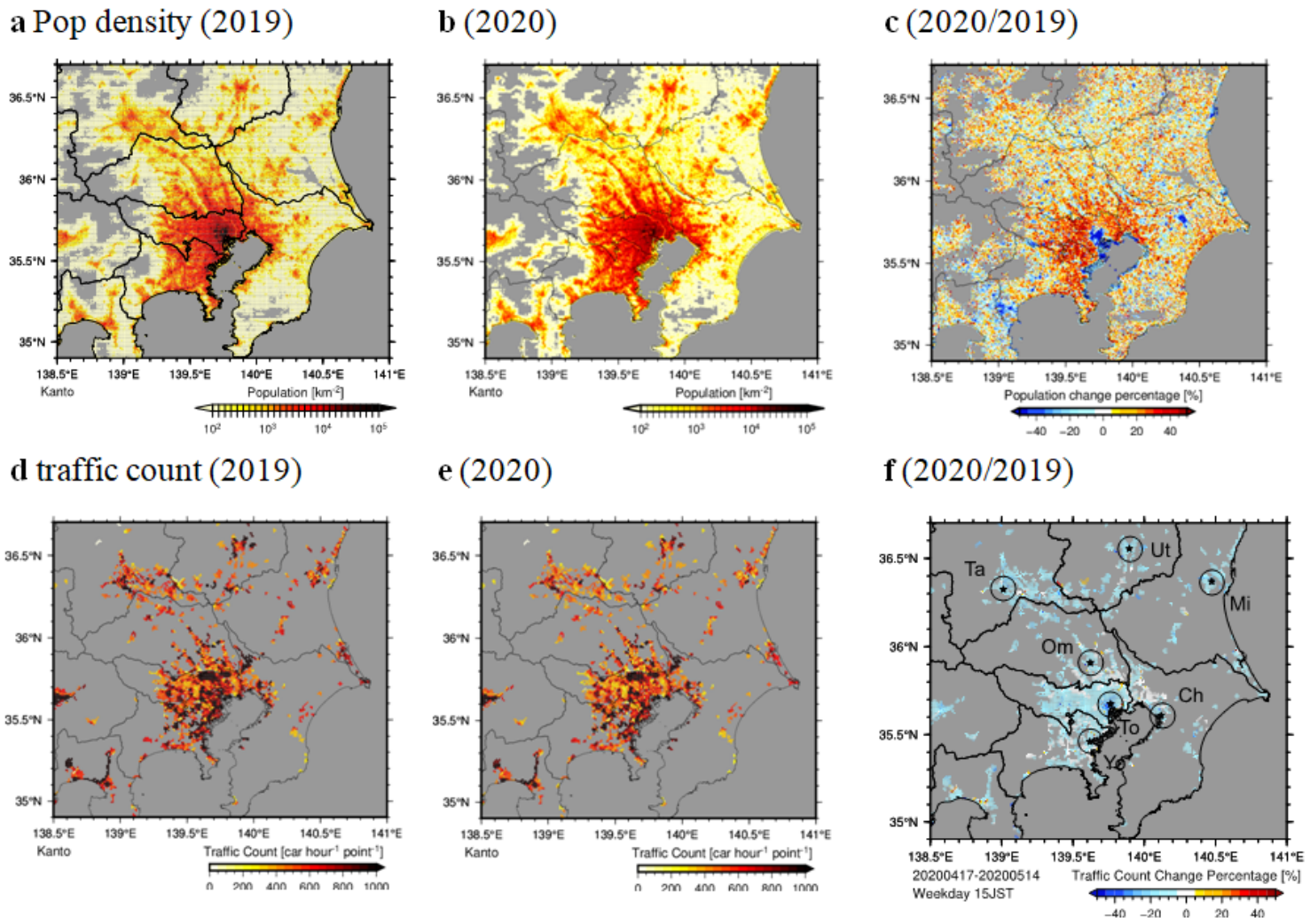

Figure 1

Changes in population (pop/km^{-2}) and traffic count (car hour^{-1} point^{-1}) on the Kanto Plain due to the COVID-19 pandemic, including the Tokyo Metropolitan Area (TMA). Horizontal variation in population densities for 15:00 Japan Standard Time (JST) 18 April–14 May 2019 (**a**), 2020 (**b**), and the 2020/2019 change ratio (**c**). Traffic counts for 18 April–14 May 2019 (**d**), 2020 (**e**), and the 2020/2019 change ratio (**f**). To (Tokyo), Yo (Yokohama), Ch (Chiba), Om (Omiya), Mi (Mito), Ta (Takasaki), and Ut (Utsunomiya).

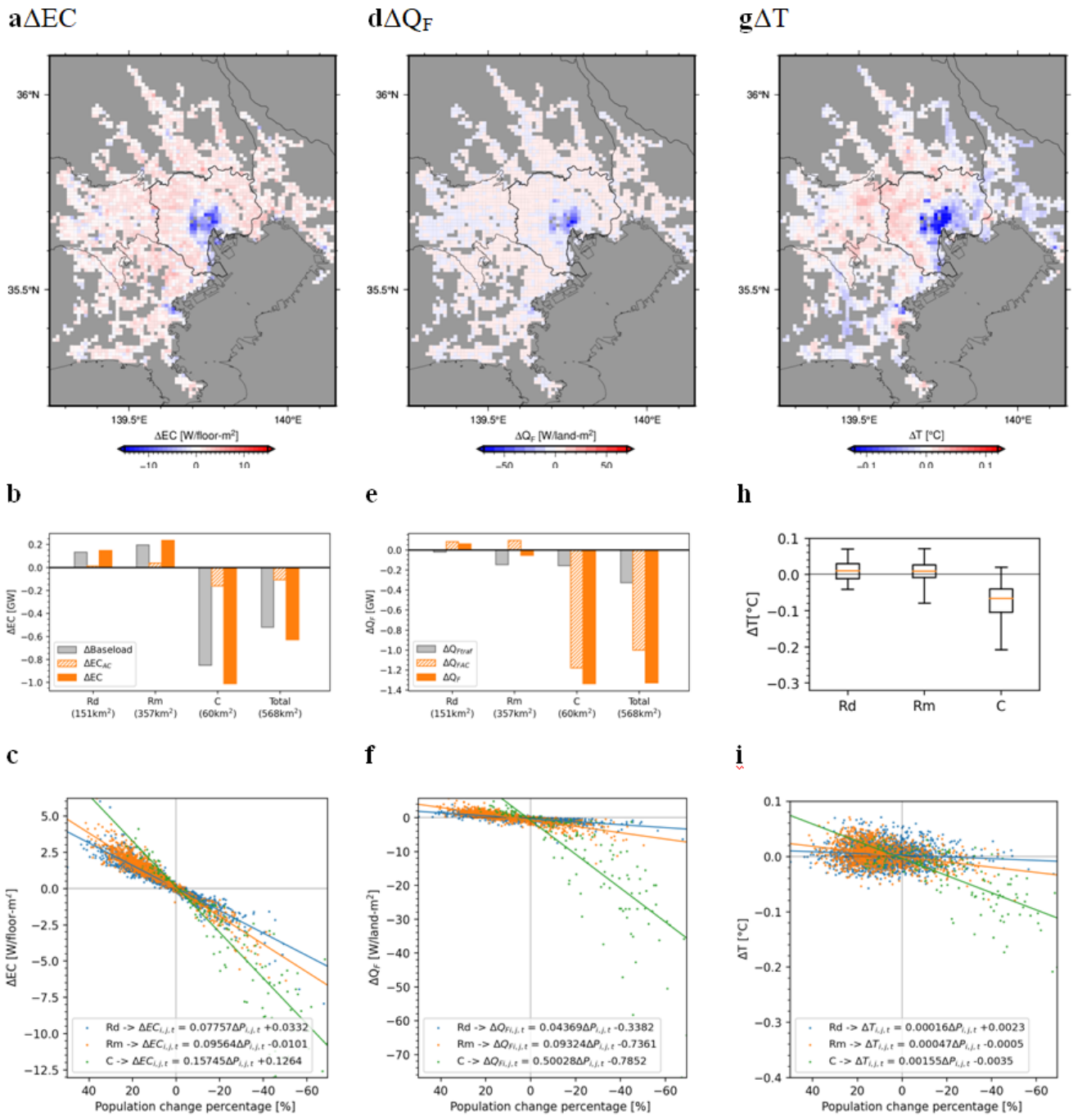

Figure 2

Impact of COVID-19 on urban climate. Horizontal variation in the impact of COVID-19 on energy consumption (EC) (**a**: ΔEC), anthropogenic heat (Q_F) (**d**: ΔQ_F) and near-surface air temperature (T) (**g**: ΔT) as a daytime average for the period of 18 April–14 May 2020. Bar charts and box plots of ΔEC (**b**), ΔQ_F (**e**) and ΔT (**h**) for each urban category and the total for the 23 wards of Tokyo (black line in **a**, **d**, and **g**). The relationship between population change and ΔEC (**c**), ΔQ_F (**f**) and ΔT (**i**) for each urban category.

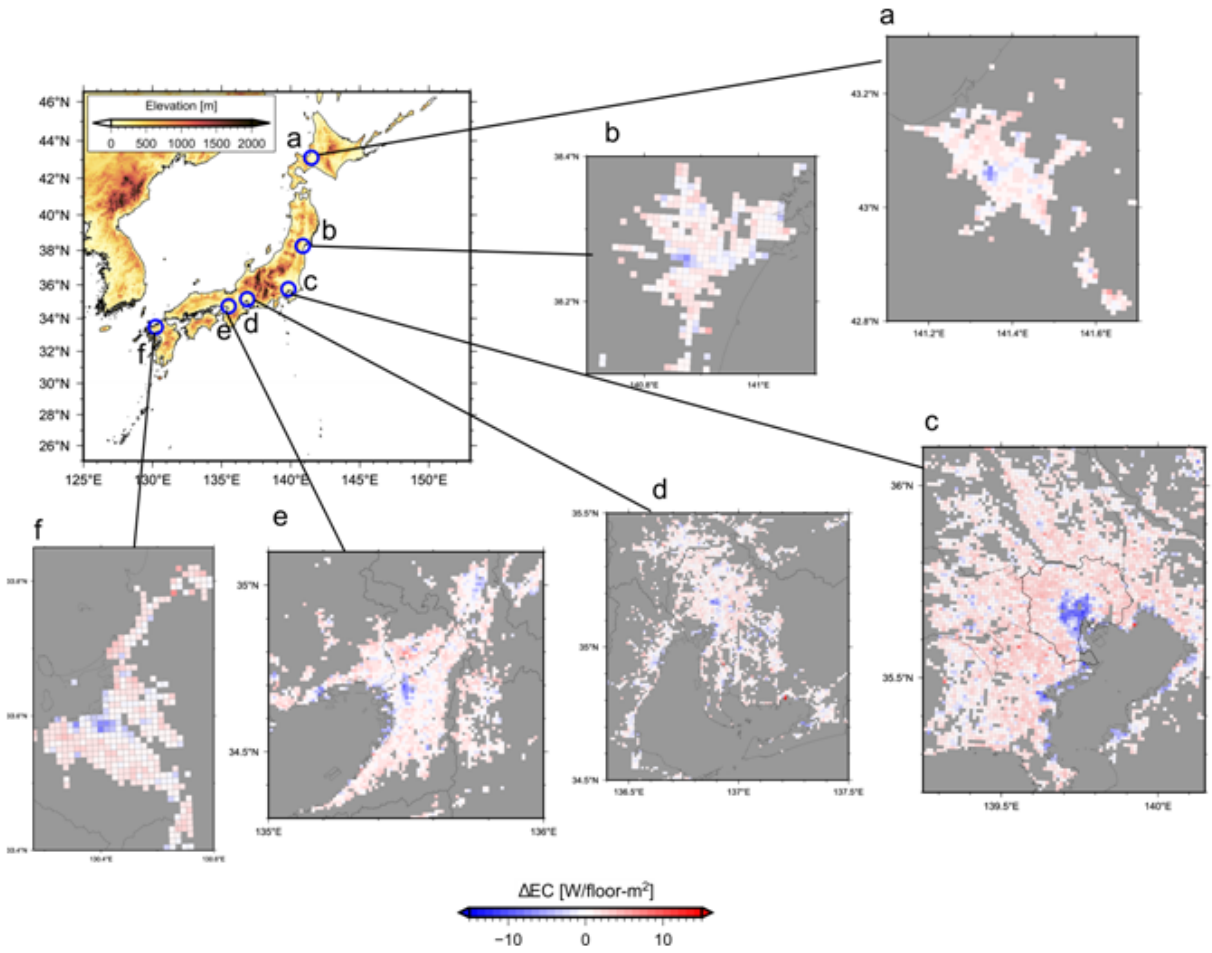

Figure 3

Estimated change in energy consumption (ΔEC) for six major metropolises in Japan: **a** Sapporo (Hokkaido), **b** Sendai (Miyagi), **c** Tokyo (TMA), **d** Nagoya (Aichi), **e** Osaka (Osaka), Kyoto (Kyoto) and Kobe (Hyogo), and **f** Fukuoka (Fukuoka).

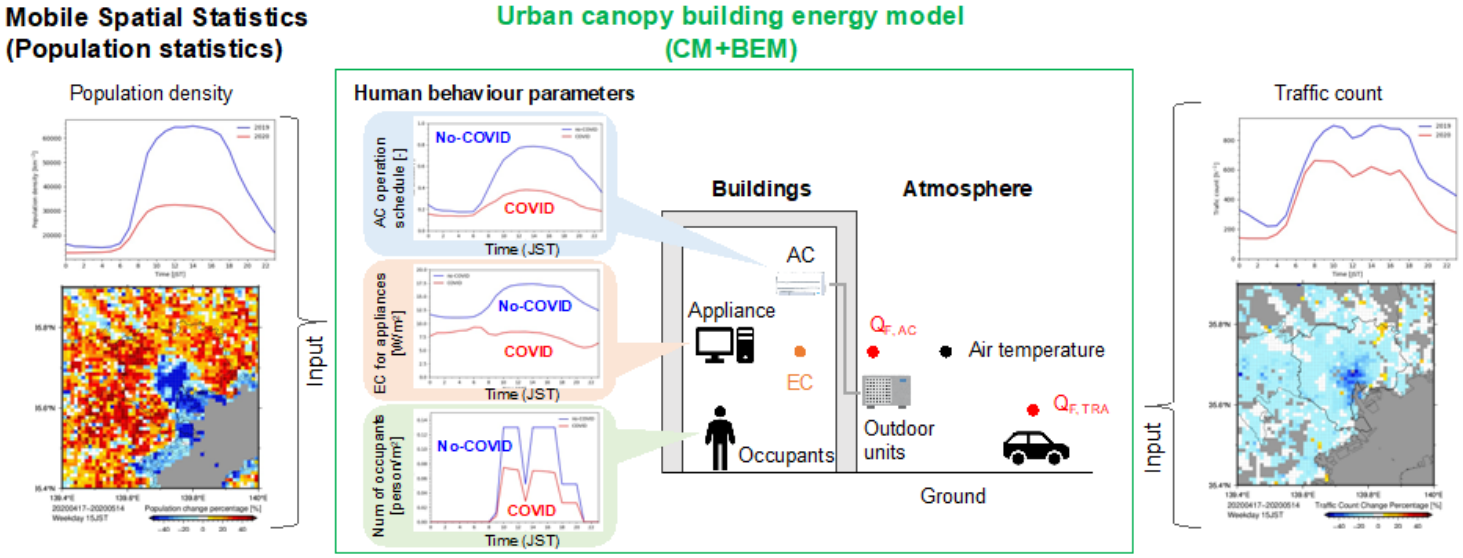

Figure 4

Schematic view of the COVID and No-COVID cases using an urban canopy building energy model (UCM-BEM), mobile spatial statistics (MSS) and traffic count data.

Supplementary Files

This is a list of supplementary files associated with this preprint. Click to download.

- Supplementalmaterial220209.docx